https://doi.org/10.15407/ujpe68.8.543

S. STARYI,[1] I. LYSJUK,[1] O. GOLENKOV,[1] Z. TSYBRII,[1] S. DANILOV,[2]
J. GUMENJUK-SICHEVSKA,[1] K. ANDRIEIEVA,[1] M. SMOLII,[1] F. SIZOV [1]

[1] V.E. Lashkaryov Institute of Semiconductor Physics, Nat. Acad. of Sci. of Ukraine
(41, Prosp. Nauky, Kyiv 03680, Ukraine)
[2] Terahertz Center, University of Regensburg
(93040 Regensburg, Germany)

CARRIER DECAY LIFETIMES IN THE NARROW-GAP $\mathbf{Hg_{1-x}Cd_xTe}$ AT THE INTERBAND AND INTRABAND EXCITATIONS

The lifetimes of photoconductive decay carriers under interband and intraband excitations are studied in epitaxial layers of narrow-gap $Hg_{1-x}Cd_xTe$ ($x \sim 0.2$). Samples with large distances (>3 mm) between small-area electrical contacts and small distances ($\sim$10 μm) with large-area contacts (THz antennas) are studied. The lifetimes of decay carriers for intraband and interband excitations are measured and compared. It has been established that, in samples with n-type conductivity, the lifetimes are comparable (in the interval of 40 ns) for both methods of excitation. At the same time, in samples with a small distance between contacts and a large area (bow-tie antennas), contacts make the main contribution to recombination. The elimination of recombination at the contacts leads to a lifetime of $\sim 10^{-6}$ s.

Keywords: HgCdTe, lifetime, interband and intraband excitations, terahertz radiation.

1. Introduction

The mercury-cadmium-telluride (MCT, HgCdTe) solid solutions are within the most studied semiconductors and have found an important application in the infrared (IR) device technology. The physics and applications of the $Hg_{1-x}Cd_xTe$ IR detectors and systems were summarized in a number of review papers and books (see, e.g., [1–4]). The mechanisms of the recombination of excess carriers in these semiconductors have an important influence on IR detectors and, to a large extent, control their performance [3, 5, 6]. Despite the fact that these mechanisms in $Hg_{1-x}Cd_xTe$ ($x \sim 0.2$ and $x \sim 0.3$) materials, as well as in devices based on them, have been intensively studied by various experimental methods [7–9], the values of the lifetime published in the literature have ranged from micro- to nanoseconds. The fact is that the lifetime of excess carriers critically depends on the quality of materials prepared by different techniques, technology of IR devices on their base, and methods of its measurement.

Under the condition of weak excitation, the effective total lifetime of excess carriers is determined by several recombination mechanisms [1]:

$$\tau_{\rm tot}^{-1} = \tau_{\rm bulk}^{-1}+\tau_{\rm surf}^{-1} = \tau_{A1}^{-1}+\tau_{A7}^{-1}+\tau_{\rm rad}^{-1}+\tau_{\rm SRH}^{-1}+\tau_{\rm surf}^{-1}, \quad (1)$$

Citation: Staryi S., Lysjuk I, Golenkov O., Tsybrii Z., Danilov S., Gumenjuk-Sichevska J., Andrieieva K., Smolii M., Sizov F. Carrier decay lifetimes in the narrow-gap $Hg_{1-x}Cd_xTe$ at the interband and intraband excitations. *Ukr. J. Phys.* **68**, No. 8, 543 (2023). https://doi.org/10.15407/ujpe68.8.543.

Цитування: Старий С., Лисюк І., Голенков О., Цибрій З., Данілов С., Гуменюк-Сичевська Ж., Андрєєва К., Смолій М., Сизов Ф. Часи життя носіїв заряду у вузькощілинному $Hg_{1-x}Cd_xTe$ при міжзонному та внутрішньозонному збудженні. *Укр. фіз. журн.* **68**, №8, 545 (2023).

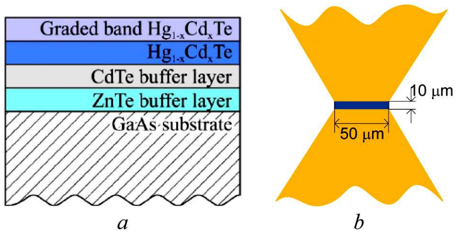

Fig. 1. Schematic cross section of investigated samples of MBE grown MCT layers (*a*) and bow-tie antenna with MCT sensitive area (*b*) [21]

where $\tau_{\rm bulk}$ and $\tau_{\rm surf}$ are the recombination times in the bulk and at the surface of the semiconductor (here, at contacts), respectively, τ_{A1} and τ_{A7} are the $A1$ and $A7$ interband Auger recombination mechanisms, $\tau_{\rm rad}$ is the interband radiative recombination mechanism, $\tau_{\rm SRH}$ is the Shockley–Read–Hall (SRH) recombination via the states in the gap. It is assumed that the Auger and radiative mechanisms are fundamental, while SRH and surface recombination depend on the technologies of manufacturing the materials and devices [1].

The Auger $A1$ and $A7$ recombination mechanisms are mainly considered for narrow-gap semiconductors (as HgCdTe or InSb). For their realization, the lowest threshold energy is required [10, 11]. The Auger processes play an important role in limiting the performance of HgCdTe infrared photodiodes, especially when the energy band-gap is decreased, and the temperature is increased [1, 2, 4]. The Shockley–Read–Hall recombinationis are most important at low temperatures. A number of deep levels of intrinsic defects and impurities, which may be responsible for this mechanism, were found for HgCdTe(see, e.g., [3, 8, 12–13]). With a sufficient decrease in the concentration of SRH recombination centers, this mechanism together with the radiative mechanism remain the fundamental limitation mechanism for the lifetime of minority carriers, which defines the upper feasible device parameters [3, 6].

Among a large variety of methods [14] of getting the lifetime of excess carriers, the different decay methods seem to be the most frequently applied. In these methods, the excess carriers are generated by a pulse of light with a turn-off time (falling time) shorter than the lifetime to be measured. The photoconductivity decay time can be measured by the direct observation of the resistivity or by the microwave method (reflection or absorption of decaying free carrier concentrations in a microwave spectral region) (see, e.g., [15–18]. The conductivity changes due to excess carriers excited by the microwave power were previously used for measuring the lifetime of excess carriers in n-type and p-type $Hg_{1-x}Cd_xTe$ with $x = 0.22$ and 0.3 [19]. The photoconductivity decay was monitored by measuring the microwave reflection. The important advantage of this method is that the samples need no special preparation, and the contact-resistance effects are eliminated. The lifetime values obtained by the microwave reflection were found to agree well with those obtained by the conventional photoconductive decay over a wide range of lifetimes. However, the microwave reflection technique requires the prior application of surface passivation and, in fact, does not account for the influence of contacts on the value of lifetimes for the intraband excitation.

The goal of this research is the investigation of the decay carrier lifetime τ under the interband (the band-gap $E_g < h\nu$, where $h\nu$ is the energy of a photon under the excitation) and intraband (the band-gap $E_g \gg h\nu$) radiation excitations in HgCdTe photoconductors with various distances between the electrical contacts and various areas of contacts. In the case of the interband excitation, the decay of excess carriers is observed as a change in the voltage on the load resistance. In this work, the measurements were carried out in the photoconductivity mode in order to study the effect of metal contacts on the recombination mechanism. In the samples with small distances between large-area contacts, the increase in the recombination rates at contacts can arise leading to the shortening of the decay times. An investigation of the minority carrier lifetime in HgCdTe with different geometries of electrical contacts is of importance for the design of IR photoresistors, photodiodes, and THz detectors devices.

2. Experiment and Discussion

The $Hg_{1-x}Cd_xTe$ ($x \approx 0.2$) compensated single crystal films used for measuring the decay lifetimes were grown by the molecular beam epitaxy (MBE) on GaAs (013) substrates (see Fig. 1, *a*) [20].

The thickness of the infrared (IR) photosensitive layers with the composition $x \approx (0.20–0.22)$ was $d \approx (2.5–9.0)$ μm between ZnTe (0.01 μm) and CdTe (5–7 μm) buffer layers and a thin intermediate layer with changing the chemical composition to

$x \approx 0.2$ for eliminating the large lattice mismatch between the HgCdTe photosensitive layer and (013) GaAs substrate. To protect the photosensitive layers, the cover layers with variable composition gradient (up to $x \approx 0.5$ and thickness $D \approx 0.9$ μm) were grown. This creates the electric field preventing the charge–carrier recombination at the interface and a surface leakage current suppression [20]. The typical electron mobility in the as-grown wafer was within $\mu \sim (6–9) \times 10^4$ cm^2/V·s. The recombination times $\tau \approx (0.8–2)$ μs were obtained from contactless SHF (super high frequency, cm wave-band) radiation reflection decay measurements in large-area wafers. The excess carriers were generated by a GaAs laser ($\lambda \approx 0.92$ μm) [22]. The estimated intrinsic concentrations for these layers with $x \approx 0.20–0.22$ are: $n_i(80\ \mathrm{K}) \approx (1.2–0.2) \times 10^{14}$ cm^{-3} for the band-gap $E_g \approx (0.084–0.11)$ eV and $n_i(300\ \mathrm{K}) \approx (6.0–2.0) \times 10^{16}$ cm^{-3} for the band-gap $E_g \approx (0.155–0.18)$ eV. There were chosen for the samples with relatively high intrinsic concentrations N_i, to satisfy the conditions of free-carrier THz or microwave response in MCT photoconductors [23].

For measuring the decay time under the interband radiation excitation, we used the samples with long distance between the electrical contacts to exclude their influence on the carrier lifetime. For measuring the decay recombination time in the THz or microwave spectral regions (intraband excitation), only small-width sensitive layers ($d \approx 10$ μm) with metal contacts in the form of bow-tie antennas to introduce the radiation into the samples were used. To study the influence of electrical contacts on recombination times, the large-area contacts (antennas, Mo/In or Mo/Au) were deposited on the active layers. To introduce an electromagnetic radiation in THz and microwave spectral ranges ($E_g \gg h\nu$), cap dielectric layers were deleted by the wet etching in a bromine-methanol solution.

2.1. Decay carrier lifetime at the intraband excitation

In the decay lifetime experiments, we used the samples with bow-tie antennas with the spacing between blades $d \approx 10$ μm (Fig. 1, *b*). Blades were obtained by the dc magnetron sputtering of thin ($d \sim 700$ A) molybdenum adhesive layers and the subsequent evaporation of $d \sim 1$ μm indium or gold contact blade layers on MCT sensitive layers obtained by the wet chemical etching of cap protective graded band layers (Fig. 1, *a*). The dimensions of blade layers were about 2 mm in length used as antennas to let the microwave radiation ($\nu \approx 70.05$ GHz) or THz radiation (high-power THz molecular lasers pumped by a transverse excited atmospheric TEA-CO_2 with $h\nu = 0.617$ and 1.07 THz), to be introduced in the MCT sensitive layers of the area $A \approx 10 \times 50$ μm.

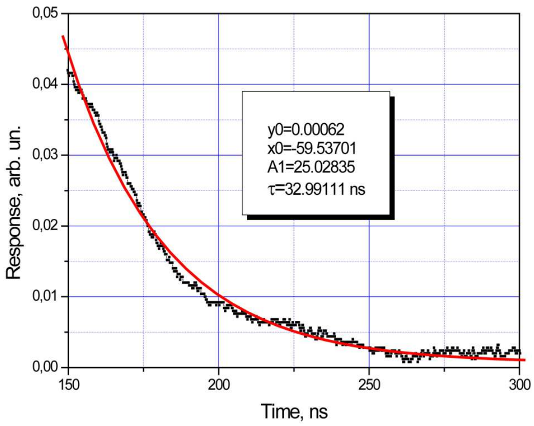

Fig. 2. The decay curve of photoresponse after the intraband radiation excitation in the photoconductor with n-type conductivity, $N(80\ \mathrm{K}) \approx 1.4 \times 10^{14}$ cm^{-3}. The radiation frequency $\nu = 70.05$ GHz, $T \approx 80$ K. The duration of a power impulse from the microwave IMPATT source was about 100 ns, the rise and fall times were not more than 5 ns. The distance between contacts-antennas is $\approx$10 μm (Fig. 1). The symbols (black line) are the experimental photoresponse. The calculated decay time of photoresponse (solid red line) is $\tau \approx 30$ ns. The decay times (time-dependent sample resistance) was measured by a TDS2022 Tektronix oscilloscope (analogous bandwidth of 200 MHz, the rise time $\leqslant$2.1 ns)

For the excitation we used the microwave IMPATT (impact ionization avalanche transit-time) diode source with the radiation frequency $\nu \approx 70.05$ GHz ($h\nu \approx 2.9 \times 10^{-4}$ eV $\ll E_g$) and the impulse duration of (80–100) ns, with the rise and falling times of not more than 5 ns. We applied bow-tie antennas designed for the frequency range $\nu \sim 300$ GHz the gain of which for this radiation frequency range is $G \ll 1$. This means that only a small part of the power $P \approx 3.8$ W from the microwave emitter was introduced into the samples. The distribution of the power density I in the sample plane is close to the Gauss one and can be approximated by $I(r) = I_0 \exp\left(-\frac{r^2}{r_0^2}\right)$, where r is the radial distance,

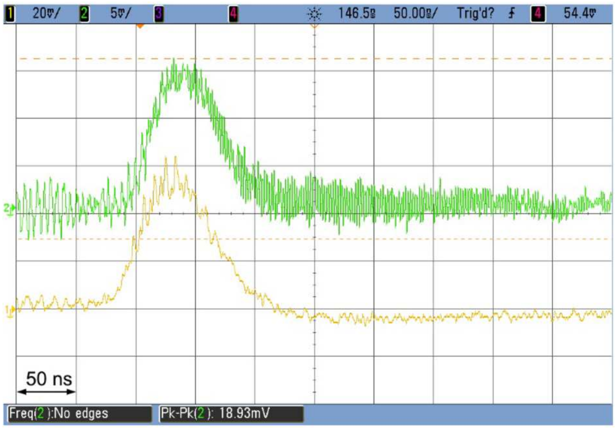

Fig. 3. The laser pulse and response time in a photoconductive compensated single crystal $Hg_{0.799}Cd_{0.201}Te$ film, n-type conductivity, $N(80\ \text{K}) \approx 1.4 \times 10^{14}\ \text{cm}^{-3}$. $T = 300$ K, $\lambda = 486\ \mu$m ($\nu = 0.617$ THz). Yellow line (*1*) represents the laser impulse, and the green line (*2*) corresponds to the MCT free-carrier photoconductor response. The distance between contacts-antennas is ≈10 μm (Fig. 1)

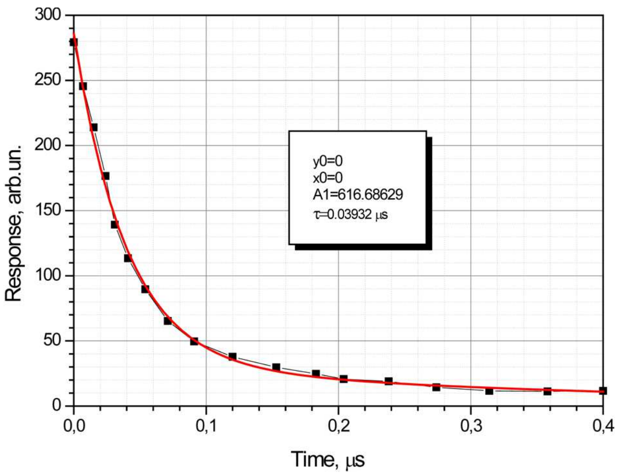

Fig. 4. The decay curve of photoresponse after the interband radiation excitation in the photoconductor with n-type conductivity, $N(80\ \text{K}) \approx 1.4 \times 10^{14}\ \text{cm}^{-3}$. $T \approx 80$ K. Semiconductor GaAs laser, $\lambda = 0.88\ \mu$m, the impulse duration ∼70 ns, the light pulse (at the level of 0.1) was about 30 ns. Oscilloscope C1-70, bandwidth 50 MHz, rise time ∼7 ns. The distance between contacts-antennas is ≈10 μm (Fig. 1). The black squares are the experimental photoresponse and the calculated decay time (Eq. (1)) (solid red line) is $\tau \approx 39.3$ ns

$r_0 \approx 4$ mm, $I_0 = P/(\pi r_0^2) \approx 7.6\ \text{W/cm}^2$. The detector load for both spectral ranges was 50 Ω. For this spectral range, the decay times are well described by one time constant $\tau \approx 33$ ns (Fig. 2).

The decay time can be well described by the equation

$$y = y_0 + A_1\, e^{(t - x_0)/\tau}, \tag{2}$$

where $y_0 = 0.00062$, $x_0 = -59.5$ ns, $A_1 = 25.02835$, and $\tau = 32.9$ ns is the decay time.

As it was shown in [23, 24], the electron heating by electromagnetic waves in bipolar $Hg_{1-x}Cd_xTe$ can be used for the designing of THz/sub-THz detectors. The free-carrier photoresponse in the THz and microwave spectral ranges of MCT layersis is related to several mechanisms [24, 25]: the Dember effect (photodiffusion effect) contribution, the thermoelectromotive contribution, and the contribution associated with free carrier concentration changes.

At the intraband excitation, the observed lifetimes are changing within the different ranges of several tenths ns with the mean, over 8 samples, $\tau \sim 43$ ns. This value of the lifetime explains the form of a response of such samples showing a reiteration of the impulse duration, which, for example, for a laser operating at $\lambda = 280\ \mu$m (1.07 THz) was at least of $\tau \sim 100$ ns. The data on the response time under the gas laser excitation at the wavelengths $\lambda = 280\ \mu$m (1.07 THz) and $\lambda = 486\ \mu$m ($\nu = 0.617$ THz) were obtained for samples at $T = 300$ K (see Fig. 3).

2.2. Decay carrier lifetime at the interband excitation

For the interband excitation of MCT sensitive structures, we used an GaAs laser diode operating at the wavelength $\lambda = 0.88\ \mu$m ($h\nu = 1.41\ \text{eV} \gg E_g$ (MCT) ∼0.1 eV at $T = 80$ K) with a pulse width of ≈70 ns and the fall time duration to the level 0.1 of ∼20 ns. The typical decay photoconductive curve is showing Fig. 4. The decay curves were measured by an oscilloscope with a bandwidth of 50 MHz (rise time 10 ns).

The temperature dependences of the decay lifetime of nonequilibrium charge carriers in the n- and p-type samples of MBE grown $Hg_{1-x}Cd_xTe$ with a large distance between the contacts were measured. The interband low-intensity excitation levels ($\Delta n = \Delta p \ll n_0$ (Δn and Δp are the concentrations of nonequilibrium electrons and holes, respectively, and n_0 and p_0 are the concentrations of equilibrium electrons and holes) was used with a GaAs semiconductor laser ($h\nu \approx 1.4$ eV). For the n-type MCT materials, the

Auger recombination rates are determined by $A1$ process (involving two electrons and one heavy hole) [10].

In n-type MBE-grown layers ($x \approx 0.20$–0.22) with the electron concentration $N \sim (1$–$10) \times 10^{14}$ cm^{-3} with large distances between the small-area metallic contacts at the temperature range $T = 80$–300 K, the well-known recombination mechanisms take place. The CHCC (A1 Auger process) and SRH recombination (trap concentration $N_t \sim 1.5 \times 10^{14}$ cm^{-3}), are shown to be the basic recombination mechanisms. The estimations were made for the carrier concentration $N(80\text{ K}) \approx (1.2$–$0.2) \times 10^{14}$ cm^{-3} for the band-gap $E_g \approx (0.85$–$0.11)$ eV, and $N(300\text{ K}) \approx (2$–$4) \times 10^{16}$ cm^{-3} for the band-gap $E_g \approx (0.15$–$0.18)$ eV. At $T \leqslant 140$ K, the recombination times were within $\tau \approx (1$–$2) \times 10^{-6}$ s quickly falling down to $\tau \approx 10^{-7}$ s at $T \sim 250$ K in n-type samples. Calculations of the radiative recombination give much higher recombination times and were not taken into account.

In the p-type MBE-grown samples with the concentration of holes in the layers $P = (2$–$8) \times 10^{16}$ cm^{-3}, the estimated decay lifetimes at $T = 80$ K are $\tau \sim 2\times10^{-8}$ s. The CHLH Auger recombination (light hole, heavy hole, and electron involved, $A7$ Auger process) and the SRH recombination via defect states at the concentration of recombination centers $N_t \sim 3 \times 10^{15}$ cm^{-3} are the principal recombination mechanisms. At temperatures $T > 120$ K, mainly the Auger-7 process prevails. The radiative recombination plays almost no role at any temperature.

The decay lifetimes τ for samples with a short distance between the metallic contacts-antennas (Fig. 1, b), which were cut from the same MBE wafers can be evaluated only approximately as the values of τ obtained in 10 samples ($\tau \sim (25$–$40)$ ns) are approximately of the same order as the pulse width of a GaAs laser ($\sim$30 ns). They are significantly lower than the decay lifetimes ($\sim$1000 ns) in samples with long distances between the contacts. Therefore, in samples with a short distance between contacts, the recombination at contacts defines the recombination processes. The recombination lifetime estimated from (1) is at most $\sim$30 ns at the interband excitation. The mean decay lifetime measured over 10 samples is $\tau \approx 31$ ns.

3. Conclusions

The photoconductive decay carrier lifetime measurements in the narrow-gap $Hg_{1-x}Cd_xTe$ ($x \approx 0.2$) compensated single-crystal films with short distances between large-area metallic contacts ($\approx$10 μm) under the interband and intraband excitations ($E_g \gg h\nu$) are measured. These experiments have shown a significant lowering of the decay times in photoconductive compensated single-crystal films compared with those with long distances between the electrical contacts. The results obtained assume that, in the samples with short distances between the large-area (bow-tie antennas) contacts, the decay carrier lifetimes are influenced by the surface recombination at contacts, giving the decay times $\sim$30 times shorter compared to the samples with long distances between the contacts. The obtained results concerning an establishing lifetimes and the ratio between them for interband and intraband excitations are important for creating the dual-spectral detectors based on HgCdTe for the IR and THz spectral ranges.

The authors are thankful to S.A. Dvoretsky and N.N. Mikhailov for supplying MBE-grown MCT layers on (013) GaAs substrates.

This work was partly supported by the NAS of Ukraine, project No. 0123U100458 and the Volkswagen Foundation Partnerships-Cooperation Project "Terahertz optoelectronics in novel low-dimensional narrow-gap semiconductor nanostructures" (Project No. 97738).

1. D.L. Polla, C.E. Jones. Deep level studies of $Hg_{1-x}Cd_xTe$. I: Narrow-band-gap space-charge spectroscopy. *J. Appl. Phys.* **52**, 5118 (1981).
2. Ch.W. Myles, P.F. Williams, R.A. Chapman, E.G. Bylander. Identification of defect centers in $Hg_{1-x}Cd_xTe$ using their energy level composition dependence. *J. Appl. Phys.* **57** (12), 5279 (1985).
3. K. Lishka. Deep level defects in narrow gap semiconductors. *Phys. Status Solidi B* **133**, 17 (1986).
4. R.E. Longshore. MCT properties, growth methods and characterization. In: *Handbook of Infra-Red Detection Technologies* (Elsevier, 2002).
5. W. Lei, J. Antoszewski, L. Faraone. Progress, challenges, and opportunities for HgCdTe infrared materials and detectors. *Appl. Phys. Rev.* **2**, 041303 (2015).
6. M.A. Kinch. *State-of-the-Art Infrared Detector Technology* (SPIE Press, 2014) [ISBN: 9781628412895].
7. A. Rogalski. *Infrared and Terahertz Detectors* (CRC Press, Boca Raton, 2019) [ISBN: 9781315271330].
8. P. Landsberg. *Recombination in Semiconductors* (Cambridge Univ. Press, 1992) [ISBN: 0521361222].
9. D. Lee, P. Dreiske, J. Ellsworth, R. Cottier, A. Chen, S. Tallaricao, A. Yulius, M. Carmody, E. Piquette, M. Zan-

dian, S. Douglaset. Law 19: The ultimate photodiode performance metric. *Proc. SPIE* **11407**, 114070X (2020).
10. A.R. Beattie. Quantum efficiency in InSb. *J. Phys. Chem. Solids* **23**, 1049 (1962).
11. S.E. Schacham, E. Finkman. Recombination mechanisms in p-type HgCdTe: Freezeout and background flux effects. *J. Appl. Phys.* **57**, 2001 (1985).
12. A. Kobayashi, O.F. Sankey, J.D. Dow. Chemical trends for defect energy levels in $Hg_{1-x}Cd_xTe$. *Phys. Rev. B* **25**, 6367 (1982).
13. W. Li, J.D. Patterson. Deep defects in narrow-gap semiconductors. *Phys. Rev. B* **50**, 14903 (1994).
14. W. M.Bullis. Measurement of carrier lifetime in semiconductors – An annotated bibliography covering the period 1949–1967. *NBS Technical Note* **465**, 1 (1968).
15. R.J. Deri, J.P. Spoonhower. Microwave photoconductivity lifetime measurements: Experimental limitations. *Rev. Sci. Instrum.* **55**, 1343 (1984).
16. M. Kunst, G. Beck. The study of charge carrier kinetics in semiconductors by microwave conductivity measurements. *J. Appl. Phys.* **60**, 3558 (1986).
17. S. Mae, T. Tawara, H. Tsuchida. Microscopic FCA System for depth-resolved carrier lifetime measurement in SiC. *Mater. Sci. Forum* **924**, 269 (2018).
18. T. Asada, Y. Ichikawa, M. Kato. Carrier lifetime measurements in semiconductors through the microwave photoconductivity decay method. *J. Vis. Exp.* **146**, e59007 (2019).
19. V.C. Lopes, A.J. Syllaios, M.C. Chen. Minority carrier lifetime in mercury cadmium telluride. *Semicond. Sci. Tech.* **8**, 824 (1993).
20. S.A. Dvoretsky, N.N. Mikhailov, V.G. Remesnik, Yu. Sidorov, V. Shvets, D. Ikusov, V. Varavin, M. Yakushev, J. Gumenjuk-Sichevska, A. Golenkov, I. Lysiuk, Z. Tsybrii, A. Shevchik-Shekera, F. Sizov, A. Latyshevetal. MBE-grown MCT hetero- and nanostructures for IR and THz detectors. *Opto-Electron. Rev.* **27**, 282 (2019).
21. F. Sizov, Z. Tsybrii, S. Danilov, N. Mikhailov, S. Dvoretsky, J. Gumenjuk-Sichevska. THz polarization-dependent response of antenna-coupled HgCdTe photoconductors under an external constant electric field. *Semicond. Sci. Tech.* **36**, 105009 (2021).
22. S.A. Dvoretsky, M.F. Stupak, N.N. Mikhailov, V.S. Varavin, V.G. Remesnik, S.N. Makarov, A.G. Elesin, A.G. Verhoglyad. New recombination centers in MBE MCT layers on (013) GaAs substrates. *Phys. Solid State* **65**, 53 (2023).
23. V. Dobrovolsky, F. Sizov. A room temperature, or moderately cooled, fast THz semiconductor hot electron bolometer. *Semicond. Sci. Tech.* **22**, 103 (2007).
24. V. Zabudsky, F. Sizov, N. Momot, Z. Tsybrii, N. Sakhno, S. Bunchuk, N. Michailov, V. Varavin. THz/sub-THz direct detection detector on the basis of electron/hole heating in MCT layers. *Semicond. Sci. Tech.* **27**, 045002 (2012).
25. V. Dobrovolsky, F. Sizov. THz/sub-THz bolometer based on electron heating in a semiconductor waveguide. *Opto-Electron. Rev.* **18**, 250 (2010).

Received 16.06.23

С. Старий, І. Лисюк, О. Голенков,
З. Цибрій, С. Данілов, Ж. Гуменюк-Сичевська,
К. Андреева, М. Смолій, Ф. Сизов

ЧАСИ ЖИТТЯ НОСІЇВ
ЗАРЯДУ У ВУЗЬКОЩІЛИННОМУ
$Hg_{1-x}Cd_xTe$ ПРИ МІЖЗОННОМУ
ТА ВНУТРІШНЬОЗОННОМУ ЗБУДЖЕННІ

Досліджено часи життя спаду фотопровідності носіїв заряду при міжзонному та внутрішньозонному збудженні в епітаксійних шарах вузькощілинного $Hg_{1-x}Cd_xTe$ ($x \sim 0{,}2$). Вивчалися зразки з великими відстанями (>3 мм) між електричними контактами малої площі та малими відстанями (∼10 мкм) з контактами великої площі (ТГц антени). Часи життя носіїв заряду було виміряно при внутрішньозонному і міжзонному збудженні та зроблено порівняльний аналіз. Встановлено, що в зразках з n-типом провідності часи життя порівняні (в діапазоні 40 нс) для обох способів збудження. У той же час, у зразках з малою відстанню між контактами і великою площею (метеликоподібні антени) контакти вносять основний внесок у рекомбінацію носіїв заряду. Усунення рекомбінації на контактах приводить до збільшення часу життя $\sim 10^{-6}$ с.

Ключові слова: HgCdTe, часи життя, внутрішньозонне і міжзонне збудження, випромінення у діапазоні ТГц.